

Perturbative QCD Study of $B \rightarrow D^{(*)}$ Decays

Chung-Yi Wu¹, Tsung-Wen Yeh¹ and Hsiang-nan Li²

¹Department of Physics, National Cheng-Kung University,
Tainan, Taiwan, R.O.C.

²Department of Physics, National Chung-Cheng University,
Chia-Yi, Taiwan, R.O.C.

June 10, 2021

PACS numbers: 13.20.He, 12.15.Hh, 12.38.Bx

Abstract

We compute various form factors involved in $B \rightarrow D^{(*)}$ transitions based on the perturbative QCD formalism, which includes Sudakov effects from the resummation of large radiative corrections in a heavy-light system. A two-parameter model wave function for $D^{(*)}$ mesons is fixed using data of the nonleptonic decays $B \rightarrow D^{(*)}\pi$, from which the ratio of the decay constants $f_{D^*}/f_D = 0.92$ is obtained. We then derive the spectrum of the semileptonic decay $B \rightarrow D^*\ell\nu$ in the fast recoil region of the D^* meson, and extract the CKM matrix element $|V_{cb}| = 0.043 \times (0.12 \text{ GeV}/f_B) \times (0.14 \text{ GeV}/f_D)$, f_B and f_D being the B and D meson decay constants, respectively. Here we adopt the convention with the pion decay constant $f_\pi = 93 \text{ MeV}$. With these outcomes, we evaluate the decay rate of $B \rightarrow DD_s$, and estimate the ratio $f_{D_s}/f_D = 0.98$ from data. Contributions of internal W -emission and W -exchange diagrams are briefly discussed.

1 Introduction

Recently, the perturbative QCD (PQCD) formalism including Sudakov effects has been shown to be applicable to heavy meson decays, which were usually regarded as being dominated by nonperturbative dynamics. The breakthrough is attributed to the resummation of large radiative corrections in heavy-light systems such as a B meson containing a light valence quark. This resummation, which was first performed in [1] for the semileptonic decays $B \rightarrow \pi(\rho)\ell\nu$, improves the applicability of PQCD to these heavy-to-light transitions. It was found that PQCD predictions are reliable for the energy fraction of the pion above 0.3, from which the Cabibbo-Kobayashi-Maskawa (CKM) matrix element $|V_{ub}|$ can be extracted, once experimental data are available. A similar formalism was applied to $B \rightarrow D$ decays in the fast recoil region of the D meson [2], and found to be self-consistent for velocity transfer above 1.3. The resummation technique was further employed to study the inclusive decays $B \rightarrow X_s\gamma$ and $B \rightarrow X_u\ell\nu$ [3], and the Sudakov effects at the end points of spectra were examined [4].

In this paper we shall extend the analysis in [2], and evaluate all the form factors involved in $B \rightarrow D^{(*)}$ transitions at the high end of velocity transfer η . The B meson wave function is determined by the relativistic constituent quark model [5]. For fast $D^{(*)}$ mesons, a convincing model wave function is still not yet obtained. We propose a two-parameter $D^{(*)}$ meson wave function, and fix the parameters using data in the large η region from the nonleptonic decays $B \rightarrow D^{(*)}\pi$ [6]. One of the parameters corresponds to the normalization constant, and the other controls the shape. With these phenomenological inputs, our analysis is free of the ambiguity from nonperturbative effects. We compare our results to those from other theoretical approaches, for example, heavy quark symmetry (HQS) [7] combined with $\mathcal{O}(\alpha_s)$ and $\mathcal{O}(1/M)$ corrections in [8] and overlap integrals of heavy meson wave functions in [9, 10].

We derive the spectrum of the semileptonic decay $B \rightarrow D^*\ell\nu$ from the transition form factors. The CKM matrix element $|V_{cb}|$ is then obtained by fitting our predictions to data [11] at large η , where PQCD is reliable. Our approach to the extraction of $|V_{cb}|$ differs from those in the literature, where the behaviors of the form factors at $\eta = 1$ are employed. The relevant nonvanishing form factors take the same functional form $\xi(\eta)$, which is normalized to unity at zero recoil, $\xi(\eta = 1) = 1$, because of HQS. The quantity $|V_{cb}|\xi(1)$ can be extracted from experimental data, if the behavior of ξ above zero recoil is known. However, ξ is thought of as being uncalculable in perturbation

theory, and thus the extraction depends on how to extrapolate ξ from $\eta = 1$ to $\eta > 1$. Hence, different models of $\xi(\eta)$ lead to different values of $|V_{cb}|$ [8, 11]. We argue that ξ is in fact calculable in the fast recoil region. The nonperturbative wave functions, fixed by data of other decay modes, provide model-independent extraction of $|V_{cb}|$.

The consistency of $|V_{cb}|$ determined in this paper with currently accepted values justifies the PQCD analysis of B meson decays, especially $B \rightarrow \pi$ decays. Predictions for the spectra of the decays $B \rightarrow \pi(\rho)\ell\nu$ in [1] are then convincing, and can be used to extract $|V_{ub}|$. On the other hand, HQS requires only the normalization of heavy-to-heavy transition form factors at zero recoil. The PQCD formalism, however, gives information near the high end of η . Therefore, these two approaches complement each other. Furthermore, our formalism is applicable to the evaluation of nonfactorizable contributions from W -exchange diagrams, which remains a challenging subject in the study of nonleptonic B meson decays.

We develop the factorization formulas for all the $B \rightarrow D^{(*)}$ transition form factors in Sect. 2. In Sect. 3 the two-parameter $D^{(*)}$ meson wave function is determined by fitting the data of the decays $B \rightarrow D^{(*)}\pi$. The $B \rightarrow D^*\ell\nu$ spectrum is derived, and $|V_{cb}|$ is extracted from experimental data [11]. We show in Sect. 4 that nonfactorizable contributions from W -exchange diagrams are negligible. Sect. 5 is the conclusion.

2 Factorization Formulas

The six form factors ξ_i , $i = +, -, V, A_1, A_2$ and A_3 , involved in $B \rightarrow D^{(*)}$ transitions are defined by the following matrix elements:

$$\begin{aligned}
\langle D(P_2)|V^\mu|B(P_1)\rangle &= \sqrt{M_B M_D}(\xi_+(\eta)(v_1 + v_2)^\mu + \xi_-(\eta)(v_1 - v_2)^\mu), \\
\langle D^*(P_2)|V^\mu|B(P_1)\rangle &= i\sqrt{M_B M_{D^*}}\xi_V(\eta)\epsilon^{\mu\nu\alpha\beta}\epsilon_\nu^*v_{2\alpha}v_{1\beta}, \\
\langle D^*(P_2)|A^\mu|B(P_1)\rangle &= \sqrt{M_B M_{D^*}}[\xi_{A_1}(\eta)(\eta + 1)\epsilon^{*\mu} - \xi_{A_2}(\eta)\epsilon^* \cdot v_1 v_1^\mu \\
&\quad - \xi_{A_3}(\eta)\epsilon^* \cdot v_1 v_2^\mu].
\end{aligned} \tag{1}$$

The momentum P_1 (P_2), the mass M_B ($M_{D^{(*)}}$) and the velocity v_1 (v_2) of the B ($D^{(*)}$) meson are related by $P_1 = M_B v_1$ ($P_2 = M_{D^{(*)}} v_2$). The velocity transfer $\eta = v_1 \cdot v_2$ has been introduced before, whose expression in terms of

the momentum transfer $q^2 = (P_1 - P_2)^2$ is given by

$$\eta = \frac{M_B^2 + M_{D^{(*)}}^2 - q^2}{2M_B M_{D^{(*)}}} . \quad (2)$$

ϵ^* is the polarization vector of the D^* meson, satisfying $\epsilon^* \cdot v_2 = 0$. The vector current V^μ and the axial vector current A^μ are defined by $V^\mu = \bar{c}\gamma^\mu b$ and $A^\mu = \bar{c}\gamma^\mu\gamma_5 b$, respectively.

In the infinite mass limit of M_B and $M_{D^{(*)}}$, the six form factors have the relations

$$\xi_+ = \xi_V = \xi_{A_1} = \xi_{A_3} = \xi, \quad \xi_- = \xi_{A_2} = 0, \quad (3)$$

where ξ is the Isgur-Wise (IW) function [7] mentioned in the Introduction. ξ is normalized to unity at zero recoil from HQS. For the behavior of ξ above zero recoil, there is only model estimation from the overlap integrals of heavy meson wave functions [9, 10].

We work in the rest frame of the B meson, in which P_1 is written, using light-cone components, as $P_1 = M_B/\sqrt{2}(1, 1, \mathbf{0}_T)$, and P_2 has the nonvanishing components [2]

$$\begin{aligned} P_2^+ &= \frac{\eta + \sqrt{\eta^2 - 1}}{\sqrt{2}} M_{D^{(*)}} , \\ P_2^- &= \frac{\eta - \sqrt{\eta^2 - 1}}{\sqrt{2}} M_{D^{(*)}} . \end{aligned} \quad (4)$$

As $\eta \rightarrow 1$ with $P_2^+ = P_2^- = M_{D^{(*)}}/\sqrt{2}$, the $D^{(*)}$ meson behaves like a heavy meson. However, in the large η limit with $P_2^+ \gg M_{D^{(*)}}/\sqrt{2} \gg P_2^-$, the $D^{(*)}$ meson can be regarded as being light [2]. We argue that ξ is dominated by soft contributions in the slow $D^{(*)}$ meson limit, where the heavy meson wave functions strongly overlap, and factorization theorems fail. However, when the $D^{(*)}$ meson recoils fast, carrying energy much greater than $M_{D^{(*)}}$, $B \rightarrow D^{(*)}$ transitions are then similar to $B \rightarrow \pi$ ones [2] as stated above, and PQCD is expected to be applicable. In this paper we shall show that the PQCD formalism including Sudakov effects gives reliable predictions for ξ in the large η region.

The PQCD factorization formulas for the $B \rightarrow D$ transition form factors have been derived in [2]. Here we summarize the idea. The factorization of the matrix elements in eq. (1) into the convolution of a hard scattering amplitude with the B and $D^{(*)}$ meson wave functions is shown in fig. 1a, where the b and c quarks are represented by the thicker and thick lines, respectively. k_1 (k_2) is the momentum of the light valence quark in the B ($D^{(*)}$) meson,

satisfying $k_1^2 \approx 0$ ($k_2^2 \approx 0$). k_1 has a large minus component k_1^- , which defines the momentum fraction $x_1 = k_1^-/P_1^-$, and small transverse components \mathbf{k}_{1T} , which serve as the infrared cutoff of loop integrals for radiative corrections. Similarly, k_2 has a large component k_2^+ , defining $x_2 = k_2^+/P_2^+$, and small \mathbf{k}_{2T} .

A simple investigation shows that large logarithms arise from radiative corrections to the above factorization picture. In particular, double (leading) logarithms occur in the reducible corrections illustrated by the $\mathcal{O}(\alpha_s)$ diagrams in fig. 1b [1], when they are evaluated in axial gauge. In order to have a reliable PQCD analysis, these double logarithms must be organized using the resummation technique, which leads to the evolution of the B ($D^{(*)}$) meson wave function ϕ_B ($\phi_{D^{(*)}}$) in k_1^- (k_2^+). We quote the results as follows [2]:

$$\begin{aligned}\phi_B(x_1, P_1, b_1, \mu) &\approx \phi_B(x_1) \exp \left[-s(k_1^-, b_1) - 2 \int_{1/b_1}^{\mu} \frac{d\bar{\mu}}{\bar{\mu}} \gamma(\alpha_s(\bar{\mu})) \right], \\ \phi_{D^{(*)}}(x_2, P_2, b_2, \mu) &\approx \phi_{D^{(*)}}(x_2) \exp \left[-s(k_2^+, b_2) - s(P_2^+ - k_2^+, b_2) \right. \\ &\quad \left. - 2 \int_{1/b_2}^{\mu} \frac{d\bar{\mu}}{\bar{\mu}} \gamma(\alpha_s(\bar{\mu})) \right],\end{aligned}\tag{5}$$

where b_1 (b_2) is the Fourier conjugate variable to k_{1T} (k_{2T}), and can be regarded as the spatial extent of the B ($D^{(*)}$) meson. μ is the renormalization and factorization scale. The exponent s organizes the double logarithms from the overlap of collinear and soft divergences, and the integral, with the quark anomalous dimension $\gamma = -\alpha_s/\pi$ as the integrand, groups the remaining single ultraviolet logarithms in fig. 1b. The expression of s is very complicated, and exhibited in the Appendix.

In the resummation procedures the B meson is treated as a heavy-light system. The $D^{(*)}$ meson is, however, treated as a light-light system as indicated in eq. (5), because we concentrate on the fast recoil region [2]. The initial conditions $\phi_i(x)$ of the evolution, $i = B, D$ and D^* , are of nonperturbative origin, satisfying the normalization

$$\int_0^1 \phi_i(x) dx = \frac{f_i}{2\sqrt{3}},\tag{6}$$

with f_i the meson decay constants. The initial condition in eq. (5) should be written as $\phi(x, b, 1/b)$, and $\phi(x)$ is in fact an approximation. We have neglected the intrinsic transverse momentum dependence denoted by the argument b , and PQCD corrections proportional to $\alpha_s(1/b)$, because these two effects cancel partially [1].

The evolution of the hard scattering amplitude H from the summation of single ultraviolet logarithms is expressed as [2]

$$H(k_1^-, k_2^+, b_1, b_2, \mu) \approx H^{(0)}(k_1^-, k_2^+, b_1, b_2, t) \exp \left[-4 \int_\mu^t \frac{d\bar{\mu}}{\bar{\mu}} \gamma(\alpha_s(\bar{\mu})) \right], \quad (7)$$

where the variable t denotes the largest mass scale of H . We have approximated H by the $\mathcal{O}(\alpha_s)$ expression $H^{(0)}$, which makes sense if perturbative contributions indeed dominate. Combining the evolution in the above formula, we obtain the complete Sudakov factor e^{-S} , where the exponent S is given by

$$\begin{aligned} S(k_1^-, k_2^+, b_1, b_2) &= s(k_1^-, b_1) + s(k_2^+, b_2) + s(P_2^+ - k_2^+, b_2) \\ &\quad - \frac{1}{\beta_1} \left[\ln \frac{\ln(t/\Lambda)}{-\ln(b_1\Lambda)} + \ln \frac{\ln(t/\Lambda)}{-\ln(b_2\Lambda)} \right] \end{aligned} \quad (8)$$

with $\beta_1 = (33 - 2n_f)/12$, $n_f = 4$ being the flavor number. The QCD scale $\Lambda \equiv \Lambda_{\text{QCD}}$ will be set to 0.2 GeV below. It is easy to show that e^{-S} falls off quickly in the large b , or long-distance, region, giving so-called Sudakov suppression.

With the above brief discussion, the only thing left is to compute $H^{(0)}$ for each form factor. The calculation of $H^{(0)}$ for ξ_\pm has been performed in [2]. In a similar way we derive $H^{(0)}$ for other ξ 's. The factorization formulas for all the transition form factors in b space, with Sudakov suppression included, are listed below:

$$\begin{aligned} \xi_+ &= 16\pi\mathcal{C}_F\sqrt{M_B M_D} \int_0^1 dx_1 dx_2 \int_0^\infty b_1 db_1 b_2 db_2 \phi_B(x_1) \phi_D(x_2) \\ &\quad \times [(M_B + x_2 \zeta_+ M_D) h(x_1, x_2, b_1, b_2) + (M_D + x_1 \zeta_+ M_B) h(x_2, x_1, b_2, b_1)] \\ &\quad \times \exp[-S(k_1^-, k_2^+, b_1, b_2)], \end{aligned} \quad (9)$$

$$\begin{aligned} \xi_- &= -16\pi\mathcal{C}_F\sqrt{M_B M_D} \int_0^1 dx_1 dx_2 \int_0^\infty b_1 db_1 b_2 db_2 \phi_B(x_1) \phi_D(x_2) \\ &\quad \times \zeta_- [x_2 M_D h(x_1, x_2, b_1, b_2) - x_1 M_B h(x_2, x_1, b_2, b_1)] \\ &\quad \times \exp[-S(k_1^-, k_2^+, b_1, b_2)], \end{aligned} \quad (10)$$

$$\begin{aligned} \xi_V &= 16\pi\mathcal{C}_F\sqrt{M_B M_{D^*}} \int_0^1 dx_1 dx_2 \int_0^\infty b_1 db_1 b_2 db_2 \phi_B(x_1) \phi_{D^*}(x_2) \\ &\quad \times [(M_B - x_2 \zeta_1 M_{D^*}) h(x_1, x_2, b_1, b_2) + (M_{D^*} + x_1 \zeta_2 M_B) h(x_2, x_1, b_2, b_1)] \\ &\quad \times \exp[-S(k_1^-, k_2^+, b_1, b_2)], \end{aligned} \quad (11)$$

$$\xi_{A_1} = 16\pi\mathcal{C}_F\sqrt{M_B M_{D^*}} \int_0^1 dx_1 dx_2 \int_0^\infty b_1 db_1 b_2 db_2 \phi_B(x_1) \phi_{D^*}(x_2)$$

$$\begin{aligned} & \times [(M_B - x_2 \zeta_3 M_{D^*})h(x_1, x_2, b_1, b_2) + (M_{D^*} + x_1 \zeta_4 M_B)h(x_2, x_1, b_2, b_1)] \\ & \times \exp[-S(k_1^-, k_2^+, b_1, b_2)] , \end{aligned} \quad (12)$$

$$\begin{aligned} \xi_{A_2} = & -16\pi\mathcal{C}_F\sqrt{M_B M_{D^*}} \int_0^1 dx_1 dx_2 \int_0^\infty b_1 db_1 b_2 db_2 \phi_B(x_1) \phi_{D^*}(x_2) \\ & \times x_1 \zeta_5 M_B h(x_2, x_1, b_2, b_1) \exp[-S(k_1^-, k_2^+, b_1, b_2)] , \end{aligned} \quad (13)$$

$$\xi_{A_3} = \xi_V , \quad (14)$$

with the constants

$$\begin{aligned} \zeta_+ &= \frac{1}{2} \left[\eta - \frac{3}{2} + \sqrt{\frac{\eta-1}{\eta+1}} \left(\eta - \frac{1}{2} \right) \right] , \\ \zeta_- &= \frac{1}{2} \left[\eta - \frac{1}{2} + \sqrt{\frac{\eta+1}{\eta-1}} \left(\eta - \frac{3}{2} \right) \right] , \\ \zeta_1 &= \frac{1}{2} + \frac{\eta-2}{2\sqrt{\eta^2-1}} , \\ \zeta_2 &= \frac{1}{2\sqrt{\eta^2-1}} , \\ \zeta_3 &= \frac{2-\eta-\sqrt{\eta^2-1}}{\eta+1} , \\ \zeta_4 &= \frac{1}{2(\eta+1)} , \\ \zeta_5 &= 1 + \frac{\eta}{\sqrt{\eta^2-1}} . \end{aligned} \quad (15)$$

$\mathcal{C}_F = 4/3$ is the color factor. The function h , coming from the Fourier transform of $H^{(0)}$, is given by

$$\begin{aligned} h(x_1, x_2, b_1, b_2) = & \alpha_s(t) K_0 \left(\sqrt{x_1 x_2 \zeta M_B M_{D^*} b_1} \right) \\ & \times \left[\theta(b_1 - b_2) K_0 \left(\sqrt{x_2 \zeta M_B M_{D^*} b_1} \right) I_0 \left(\sqrt{x_2 \zeta M_B M_{D^*} b_2} \right) \right. \\ & \left. + \theta(b_2 - b_1) K_0 \left(\sqrt{x_2 \zeta M_B M_{D^*} b_2} \right) I_0 \left(\sqrt{x_2 \zeta M_B M_{D^*} b_1} \right) \right] \end{aligned} \quad (16)$$

with the constant $\zeta = \eta + \sqrt{\eta^2 - 1}$. The scale t is chosen as [2]

$$t = \max(\sqrt{x_1 x_2 \zeta M_B M_{D^*}}, 1/b_1, 1/b_2) . \quad (17)$$

Note the equality of ξ_V and ξ_{A_3} . We argue that ξ_V will differ from ξ_{A_3} , if higher-order corrections to the initial condition $H(k_1^-, k_2^+, b_1, b_2, t)$ are taken into account.

3 Determination of $|V_{cb}|$

Before proceeding to the numerical analysis of eqs. (9)-(14), we discuss how to fix the B and $D^{(*)}$ meson wave functions. For the B meson, we adopt the wave function from the relativistic constituent quark model [5], $\phi_B(x) = \int d^2\mathbf{k}_T / (4\pi)^2 \phi_B(x, \mathbf{k}_T)$, with

$$\phi_B(x, \mathbf{k}_T) = N_B \left[C_B + \frac{M_B^2}{1-x} + \frac{k_T^2}{x(1-x)} \right]^{-2}. \quad (18)$$

The normalization constant N_B and the shape parameter C_B are determined by the conditions

$$\begin{aligned} \int_0^1 dx \int \frac{d^2\mathbf{k}_T}{(4\pi)^2} \phi_B(x, \mathbf{k}_T) &= \frac{f_B}{2\sqrt{3}}, \\ \int_0^1 dx \int \frac{d^2\mathbf{k}_T}{(4\pi)^2} [\phi_B(x, \mathbf{k}_T)]^2 &= \frac{1}{2}. \end{aligned} \quad (19)$$

We obtain $N_B = 49.5 \text{ GeV}^3$ and $C_B = -27.699845 \text{ GeV}^2$ for $M_B = 5.28 \text{ GeV}$ [12] and the B meson decay constant $f_B = 0.12 \text{ GeV}$ from the lattice calculation [13]. The B meson wave function is then given by

$$\phi_B(x) = \frac{N_B}{16\pi} \frac{x(1-x)^2}{M_B^2 + C_B(1-x)}. \quad (20)$$

For the $D^{(*)}$ meson, we propose the following model, which possesses the same functional form as eq. (20),

$$\phi_{D^{(*)}}(x) = \frac{N_{D^{(*)}}}{16\pi} \frac{x(1-x)^2}{M_{D^{(*)}}^2 + C_{D^{(*)}}(1-x)}. \quad (21)$$

Equation (19) is not appropriate for the determination of $N_{D^{(*)}}$ and $C_{D^{(*)}}$, when the $D^{(*)}$ meson recoils fast [2]. Hence, we shall take an alternative approach. It is known from PQCD factorization theorems that wave functions are universal, or process-independent. It hints that we can fix the parameters using data of any $B \rightarrow D^{(*)}$ decays, such as the two-body nonleptonic decays $B \rightarrow D^{(*)}\pi$, for which factorization theorems should work best. With these phenomenological inputs at specific kinematic points $\eta = \eta_{\max}$, we then predict the behaviors of all ξ 's in a finite range of η .

We assume the vertex factorization hypothesis for the following analysis, which has been shown to be consistent with current experimental data [14].

We list the formulas for the decay rates of various $B \rightarrow D^{(*)}$ decay modes involved in our study. They are

$$\begin{aligned}
\Gamma(\bar{B}^0 \rightarrow D^+ \pi^-) &= \frac{1}{32\pi} G_F^2 |V_{cb}|^2 |V_{ud}|^2 f_\pi^2 M_B^3 \frac{(1-r^2)^3 (1-r)^2}{2r} \\
&\quad \times \left[\frac{1+r}{1-r} \xi_+(\eta_{\max}) - \xi_-(\eta_{\max}) \right]^2, \\
\Gamma(\bar{B}^0 \rightarrow D^{*+} \pi^-) &= \frac{1}{32\pi} G_F^2 |V_{cb}|^2 |V_{ud}|^2 f_\pi^2 M_B^3 \frac{(1-r^2)^5}{(2r)^3} \\
&\quad \times \left[\frac{1+r}{1-r} \xi_{A_1}(\eta_{\max}) - (r\xi_{A_2}(\eta_{\max}) + \xi_{A_3}(\eta_{\max})) \right]^2,
\end{aligned} \tag{22}$$

for the nonleptonic decays, with the constants $r = M_{D^{(*)}}/M_B$ and $\eta_{\max} = (1+r^2)/(2r)$, and

$$\begin{aligned}
\frac{d\Gamma}{dq^2} &= \frac{1}{96\pi^3} G_F^2 |V_{cb}|^2 M_B^3 r^2 (\eta^2 - 1)^{1/2} (\eta + 1)^2 \\
&\quad \times \left\{ 2(1 - 2\eta r + r^2) \left[\xi_{A_1}^2(\eta) + \frac{\eta - 1}{\eta + 1} \xi_V^2(\eta) \right] \right. \\
&\quad \left. + [(\eta - r)\xi_{A_1}(\eta) - (\eta - 1)(r\xi_{A_2}(\eta) + \xi_{A_3}(\eta))]^2 \right\}
\end{aligned} \tag{23}$$

for the spectrum of the semileptonic decay $\bar{B}^0 \rightarrow D^{*+} \ell^- \bar{\nu}$ [8]. For nonleptonic decays, there exist additional important corrections from final-state interactions with soft gluons attaching the $D^{(*)}$ meson and the pion. It has been argued that these corrections produce only single logarithms, which cancel asymptotically [2], and are thus not considered here.

We adopt $G_F = 1.16639 \times 10^{-5}$ GeV⁻² for the Fermi coupling constant, $|V_{ud}| = 0.974$ for the CKM matrix element, $M_D = 1.87$ GeV and $M_{D^*} = 2.01$ GeV for the D and D^* meson masses [12], respectively, $\tau_{B^0} = 1.53$ ps for the \bar{B}^0 meson lifetime [11], $f_\pi = 93$ MeV for the pion decay constant and $f_D = 0.14$ GeV for the D meson decay constant from the lattice calculation [13]. The four parameters we shall determine are C_D (N_D is fixed by f_D from eq. (6)), C_{D^*} , f_{D^*} (or N_{D^*} equivalently) and $|V_{cb}|$. At the same time, we have four constraints from experimental data: the branching ratios $\mathcal{B}(\bar{B}^0 \rightarrow D^+ \pi^-) = 2.9 \times 10^{-3}$ and $\mathcal{B}(\bar{B}^0 \rightarrow D^{*+} \pi^-) = 2.6 \times 10^{-3}$ [6], and the height and the profile of $d\Gamma/dq^2$ at large η , or equivalently, its values at $q^2 = M_{\pi^+}^2 \approx 0$ and at $q^2 = M_{D_s}^2$ [11], $M_{D_s} = 1.97$ GeV being the D_s meson mass [12]. In principle, we can determine the $D^{(*)}$ meson wave functions and the CKM matrix element $|V_{cb}|$ completely from the data fitting.

If there are more data from other decay modes, such as $B \rightarrow D^{(*)}D_s$, f_D can be fixed phenomenologically, and needs not to be specified at the beginning. However, these data still suffer large errors [15], and it is not practical to perform the fitting based on them. On the other hand, the data of $B \rightarrow \rho$ decays, $\mathcal{B}(\bar{B}^0 \rightarrow D^+\rho^-) = 8.1 \times 10^{-3}$ and $\mathcal{B}(\bar{B}^0 \rightarrow D^{*+}\rho^-) = 7.4 \times 10^{-3}$ [6], do not give more information than $B \rightarrow \pi$ decays, and are not employed here. This is obvious from the equality of the ratios

$$\frac{\mathcal{B}(\bar{B}^0 \rightarrow D^+\rho^-)}{\mathcal{B}(\bar{B}^0 \rightarrow D^{*+}\rho^-)} \approx \frac{\mathcal{B}(\bar{B}^0 \rightarrow D^+\pi^-)}{\mathcal{B}(\bar{B}^0 \rightarrow D^{*+}\pi^-)} \approx 1.1. \quad (24)$$

Hence, the data of $B \rightarrow \rho$ decays just lead to the ρ meson decay constant $f_\rho \approx f_\pi \times \sqrt{8.1/2.9} = 0.155$ GeV, consistent with the currently accepted value. Equation (24) is a direct consequence of the vertex factorization hypothesis for the negligible ρ meson mass. Note that the Bauer-Stech-Wirbel (BSW) method [16] gives different predictions from eq. (24), which are [6]

$$\frac{\mathcal{B}(\bar{B}^0 \rightarrow D^+\rho^-)}{\mathcal{B}(\bar{B}^0 \rightarrow D^{*+}\rho^-)} = 0.885, \quad \frac{\mathcal{B}(\bar{B}^0 \rightarrow D^+\pi^-)}{\mathcal{B}(\bar{B}^0 \rightarrow D^{*+}\pi^-)} = 1.04. \quad (25)$$

Our plan is summarized as follows:

1. Assume a set of initial values of C_D and C_{D^*} , say, $C_D = -2.9$ GeV² [2] and $C_{D^*} = -3.4$ GeV². Determine the value of f_{D^*} from the ratio $\mathcal{B}(\bar{B}^0 \rightarrow D^+\pi^-)/\mathcal{B}(\bar{B}^0 \rightarrow D^{*+}\pi^-) = 1.1$, which is independent of $|V_{cb}|$.
2. Extract $|V_{cb}|$ from the magnitude of the spectrum $d\Gamma/dq^2$ at $q^2 = M_{\pi^+}^2$ using f_{D^*} from Step 1, and the initial C_D and C_{D^*} .
3. Determine a new value of C_D from $\mathcal{B}(\bar{B}^0 \rightarrow D^+\pi^-) = 2.9 \times 10^{-3}$, and a new C_{D^*} from $d\Gamma/dq^2$ at $q^2 = M_{D_s}^2$ using f_{D^*} and $|V_{cb}|$ obtained from the above two steps.
4. Go to Step 1, starting with the new initial values of C_D and C_{D^*} .

At last, the four parameters approach their limits after a few iterations. The results are

$$\begin{aligned} C_D &= -2.6179 \text{ GeV}^2, & N_D &= 13.8 \text{ GeV}^3, & f_D &= 0.14 \text{ GeV}, \\ C_{D^*} &= -3.0421 \text{ GeV}^2, & N_{D^*} &= 14.6 \text{ GeV}^3, & f_{D^*} &= 0.129 \text{ GeV}, \\ |V_{cb}| &= 0.043. \end{aligned} \quad (26)$$

The dependence of the B and $D^{(*)}$ meson wave functions on the momentum fraction x is shown in fig. 2. ϕ_B peaks at $x \approx 0.05$, and $\phi_{D^{(*)}}$ peaks at $x \approx 0.2$, indicating that the heavier B meson is strongly dominated by soft dynamics. The profiles of ϕ_D and ϕ_{D^*} are very similar, but the maximum of

ϕ_{D^*} locates at a slightly smaller x compared to ϕ_D because of the relation $|C_{D^*}|/M_{D^*}^2 > |C_D|/M_D^2$. All these features are consistent with the expectation from the ordering of the masses, $M_B \gg M_{D^*} > M_D$. That the height of ϕ_D is larger than that of ϕ_{D^*} is due to $f_D > f_{D^*}$. Note that our prediction $f_{D^*}/f_D = 0.92$ is contrary to $f_{D^*}/f_D = 1.28$ appearing in the literature [17].

The parameters in eq. (26) lead to the branching ratios $\mathcal{B}(\bar{B}^0 \rightarrow D^+\pi^-) = 2.89 \times 10^{-3}$ and $\mathcal{B}(\bar{B}^0 \rightarrow D^{*+}\pi^-) = 2.61 \times 10^{-3}$, and the spectrum $d\Gamma/dq^2$ for the semileptonic decay $\bar{B}^0 \rightarrow D^{*+}\ell^-\bar{\nu}$ as in fig. 3, where the CLEO data from Ref. [11] are also shown. It is observed that our predictions are in good agreement with the data at low q^2 , and begin to deviate above $q^2 = 4 \text{ GeV}^2$, the slow recoil region in which PQCD is not reliable. In order to justify the PQCD analysis for $q^2 < 4 \text{ GeV}^2$, or $\eta > 1.3$ approximately, we exhibit the dependence of ξ_+ and ξ_{A_1} on the cutoff $b_c = b_1 = b_2$ for $\eta = 1.3$ in fig. 4. More than 50% of the contributions to the form factors come from the region with $b < 0.6/\Lambda$, *ie.*, $\alpha_s(1/b_c)/\pi < 0.5$.

Variation of the six transition form factors with the velocity transfer η is displayed in fig. 5. From fig. 5a, we find that the magnitudes of ξ_V , ξ_{A_1} and ξ_{A_3} are almost equal, with the relation $\xi_V = \xi_{A_3} > \xi_{A_1}$, and their behaviors are close to that of ξ_+ , corresponding to the similarity between the profiles of ϕ_{D^*} and ϕ_D . This similarity is also reflected by the fact that the ratio of ξ_V to ξ_+ is roughly the same as f_{D^*}/f_D . Contrary to fig. 5a, ξ_- and ξ_{A_2} shown in fig. 5b increase with η . ξ_- possesses a smaller slope, and is expected to become negative at low η . These features are consistent with the predictions from HQS combined with $\mathcal{O}(\alpha_s)$ and $\mathcal{O}(1/M)$ corrections in [8].

The CKM matrix element $|V_{cb}| = 0.043$ extracted here is a bit larger than recent estimations in the literature, which range from 0.035 to 0.040 [10, 11, 18]. Refer to Ref. [11] in which ξ_V , ξ_{A_1} and ξ_{A_3} were modeled by the single form factor, as indicated in eq. (3),

$$\mathcal{F}(\eta) = \mathcal{F}(1)[1 - a^2(\eta - 1) + b(\eta - 1)^2] \quad (27)$$

with the parameters $a^2 = 0.84$, $b = 0$ for a linear fit and $a^2 = 0.92$, $b = 0.15$ for a quadratic fit to experimental data. The normalization $\mathcal{F}(1) = \eta_A \xi(1) + \mathcal{O}((\Lambda/M)^2)$, where η_A is a perturbatively calculable quantity, takes the value $\mathcal{F}(1) = 0.93$ [19], $\mathcal{F}(1) = 0.89$ [20] or $\mathcal{F}(1) = 0.96$ [21]. In Ref. [10] the single form factor was expressed as the overlap integral of the B and $D^{(*)}$ meson wave functions derived from the Bethe-Salpeter equation, and was parametrized by a similar formula to eq. (27),

$$\mathcal{F}(\eta) = \eta_A \left[1 - \frac{\rho_1^2}{\eta_A}(\eta - 1) + c(\eta - 1)^{3/2} \right], \quad (28)$$

for the constants $\eta_A = 0.9942$, $\rho_1^2 = 1.279$ and $c = 0.91$. The method of overlap integrals leads to the expression [9]

$$\mathcal{F}(\eta) = \frac{2}{\eta + 1} \exp \left[-2(\rho_2^2 - 1) \frac{\eta - 1}{\eta + 1} \right], \quad (29)$$

for the constant $\rho_2 = 1.19$. In Ref. [18] the best fit to the CLEO data [11] gives the form factor

$$\mathcal{F}(\eta) = 1 - 0.81(\eta - 1). \quad (30)$$

Comparing to our results, we find that eqs. (27)-(30) are in fact close to or larger than ξ_+ as shown in fig. 6. Since our form factors involved in the decay $B \rightarrow D^* \ell \nu$ are smaller, the prediction of $|V_{cb}|$ is of course larger. If substituting ξ_+ for ξ_V , ξ_{A_1} and ξ_{A_3} in eq. (23), we shall have $|V_{cb}| \approx 0.043 \times 0.9 = 0.039$ extracted from the data, which then locates in the above range.

We explain why our form factors are smaller than those in the literature. The reason is attributed to the choice of the decay constants $f_B = 0.12$ GeV and $f_D = 0.14$ GeV at the beginning of the analysis. If f_B and f_D increase to 0.13 and 0.15 GeV, respectively, f_{D^*} will become 0.138 GeV because of the ratio $f_{D^*}/f_D = 0.92$. Here we suppose that the shape parameters C_B , C_D and C_{D^*} change only slightly. Then $|V_{cb}|$ decreases to 0.037 in order to maintain the height of the spectrum. We have confirmed this argument by following Steps 1 to 4 explicitly as stated above. Therefore, the best conclusion for our study is that we have disentangled the task of determining $|V_{cb}|$ to the extent that $|V_{cb}|$ is given, in terms of f_B and f_D , by

$$|V_{cb}| = 0.043 \times \left(\frac{0.12 \text{ GeV}}{f_B} \right) \times \left(\frac{0.14 \text{ GeV}}{f_D} \right), \quad (31)$$

for f_B and f_D varying around 0.12 and 0.14 GeV, respectively. Once the precise measurement of the decay constants f_B and f_D is performed, the CKM matrix element $|V_{cb}|$ can be fixed uniquely.

At last, we compute the branching ratio $\mathcal{B}(\bar{B}^0 \rightarrow D^+ D_s^-)$ inserting the parameters in eq. (26), and compare results with the data 8.0×10^{-3} [12], if ignoring the errors. The expression for the decay rate is written as

$$\begin{aligned} \Gamma(\bar{B}^0 \rightarrow D^+ D_s^-) &= \frac{1}{32\pi} G_F^2 |V_{cb}|^2 |V_{cs}|^2 f_{D_s}^2 M_B^3 (1 - r^2)^2 \sqrt{\eta_{\max}^2 - 1} \\ &\times \left[\frac{(1+r)^2 - r'^2}{1+r} \xi_+(\eta_{\max}) - \frac{(1-r)^2 - r'^2}{1-r} \xi_-(\eta_{\max}) \right]^2, \end{aligned} \quad (32)$$

for the CKM matrix element $|V_{cs}| = 1$ [12], $r' = M_{D_s}/M_B$ and $\eta_{\max} = (1 + r^2 - r'^2)/(2r)$. We obtain the D_s meson decay constant $f_{D_s} = 0.137$ GeV, or in terms of the ratio, $f_{D_s}/f_D = 0.98$. Because of the large errors associated with the data, we do not compare this ratio with those from the lattice calculation [13] and from QCD sum rules [22], which are about 1.1 and 1.2, respectively. However, our prediction is in agreement with the simple formula [23]

$$\frac{f_{D_s}}{f_D} = \left(\frac{M_D}{M_{D_s}} \right)^2 \frac{m_c + m_s}{m_c + m_d} \approx 0.98 \quad (33)$$

for the current quark masses $m_d = 10$ MeV, $m_s = 150$ MeV and $m_c = 1.5$ GeV. Equation (33) was obtained using general arguments from the Wigner-Eckart theorem and assuming that chiral symmetry is only broken by quark mass terms.

4 Nonfactorizable Contributions

In the study of $B \rightarrow D^{(*)}$ decays, we have considered only factorizable contributions from external W -emission diagrams as in fig. 1a. For the nonleptonic decay $\bar{B}^0 \rightarrow D^+\pi^-$, there are also nonfactorizable contributions from W -exchange diagrams as shown in fig. 7a. To justify our study, we should have a convincing argument that such nonfactorizable contributions are indeed unimportant. A simple investigation shows that the PQCD formalism can be applied to fig. 7a equally well, with the following modifications:

1. The color flow in fig. 7a differs from that in fig. 1a. This distinction leads to a factor 1/3 for nonfactorizable contributions.
2. From the viewpoint of factorization theorems, fig. 7a is a crossing in the s and t channels of fig. 1a, excluding the color flow. That is, these two diagrams are similar to each other, except the interchange of the B meson and pion kinematic variables. Hence, the hard gluon propagator in fig. 7a is proportional to $1/x_3x_2$, x_3 being the momentum fraction of the pion, which comes from the replacement of x_1 by x_3 in the gluon propagator $1/x_1x_2$ associated with fig. 1a. Since x_1 and x_3 are of order 0.05 and 0.5, respectively, from the B meson and pion wave functions, the interchange leads to a factor 1/10.

Certainly, the presence of k_T^2 in the hard scatterings moderates the difference.

Therefore, we estimate that nonfactorizable contributions from W -exchange diagrams are roughly 5% of factorizable ones, and the neglect of fig. 7a is reasonable.

With the parameters determined in Sect. 3, we can also study charged B meson decays, such as $B^- \rightarrow D^0 \pi^-$, based on the PQCD formalism employed here. In this case there are additional contributions from internal W -emission diagrams as shown in fig. 7b. Following the similar reasoning, the hard scattering associated with fig. 7b, which is proportional to $1/x_1 x_3$, is obtained by interchanging the kinematical variables of the D meson and of the pion. This interchange gives a factor $0.2/0.5 = 2/5$. We estimate that contributions from internal W -emission diagrams, combined with the color-suppressing factor $1/3$, are roughly 15% of factorizable ones, which are of course sizable. This conclusion is consistent with predictions from the BSW method [6]. We shall discuss these subjects in details in a separate work [24].

5 Conclusion

In this paper we have fixed the $D^{(*)}$ meson wave function using the experimental inputs from the nonleptonic decays $B \rightarrow D^{(*)} \pi$, and evaluated the spectrum of the semileptonic decay $B \rightarrow D^* \ell \nu$ at large velocity transfer, from which the CKM matrix element $|V_{cb}| = 0.043$ is extracted. The form factors involved in $B \rightarrow D^{(*)}$ transitions are obtained, and compared to the predictions from HQS combined with $\mathcal{O}(\alpha_s)$ and $\mathcal{O}(1/M)$ corrections [8], from the overlap integrals of heavy meson wave functions [9, 10], and from the data fitting [11]. The value of $|V_{cb}|$ extracted here is larger than those in the literature [10, 11, 18], and the reason is that we have adopted the smaller decay constants f_B and f_D . A precise measurement of f_B and f_D in the future will remove this ambiguity.

We emphasize that the behaviors of all the transition form factors are derived from the single $D^{(*)}$ meson wave function that is fixed at specific kinematic points, without resorting to a model for each form factor, such as the algebraic forms employed in [19], the pole forms in [16, 25] and the exponential forms in [26]. Note that all the above model form factors are larger than ξ_+ presented in this work. Hence, they lead to smaller values of $|V_{cb}|$, ranging from 0.032 to 0.038. Our formalism, based on the parameters

in eq. (26), can be used to study B meson decays, especially the nonleptonic cases with nonfactorizable contributions, in a less ambiguous way [24].

We thank H.Y. Cheng and P. Kroll for useful discussions. This work was supported by National Science council of R.O.C. under the Grant No. NSC-85-2112-M-194-009.

Appendix

In this appendix we present the explicit expression of the exponent $s(k, b)$ appearing in eq. (5). The full expression, instead of the first six terms [27], is adopted in this paper. It is given, in terms of the variables,

$$\hat{q} \equiv \ln(k/\Lambda), \quad \hat{b} \equiv \ln(1/b\Lambda) \quad (34)$$

by [2]

$$\begin{aligned} s(k, b) = & \frac{A^{(1)}}{2\beta_1} \hat{q} \ln\left(\frac{\hat{q}}{\hat{b}}\right) - \frac{A^{(1)}}{2\beta_1} (\hat{q} - \hat{b}) + \frac{A^{(2)}}{4\beta_1^2} \left(\frac{\hat{q}}{\hat{b}} - 1\right) \\ & - \left[\frac{A^{(2)}}{4\beta_1^2} - \frac{A^{(1)}}{4\beta_1} \ln\left(\frac{e^{2\gamma-1}}{2}\right) \right] \ln\left(\frac{\hat{q}}{\hat{b}}\right) \\ & + \frac{A^{(1)}\beta_2}{4\beta_1^3} \hat{q} \left[\frac{\ln(2\hat{q}) + 1}{\hat{q}} - \frac{\ln(2\hat{b}) + 1}{\hat{b}} \right] \\ & + \frac{A^{(1)}\beta_2}{8\beta_1^3} [\ln^2(2\hat{q}) - \ln^2(2\hat{b})] \\ & + \frac{A^{(1)}\beta_2}{8\beta_1^3} \ln\left(\frac{e^{2\gamma-1}}{2}\right) \left[\frac{\ln(2\hat{q}) + 1}{\hat{q}} - \frac{\ln(2\hat{b}) + 1}{\hat{b}} \right] \\ & - \frac{A^{(1)}\beta_2}{16\beta_1^4} \left[\frac{2\ln(2\hat{q}) + 3}{\hat{q}} - \frac{2\ln(2\hat{b}) + 3}{\hat{b}} \right] \\ & - \frac{A^{(1)}\beta_2}{16\beta_1^4} \frac{\hat{q} - \hat{b}}{\hat{b}^2} [2\ln(2\hat{b}) + 1] \\ & + \frac{A^{(2)}\beta_2^2}{1728\beta_1^6} \left[\frac{18\ln^2(2\hat{q}) + 30\ln(2\hat{q}) + 19}{\hat{q}^2} - \frac{18\ln^2(2\hat{b}) + 30\ln(2\hat{b}) + 19}{\hat{b}^2} \right] \\ & + \frac{A^{(2)}\beta_2^2}{432\beta_1^6} \frac{\hat{q} - \hat{b}}{\hat{b}^3} [9\ln^2(2\hat{b}) + 6\ln(2\hat{b}) + 2] . \end{aligned} \quad (35)$$

The above coefficients β_i and $A^{(i)}$ are

$$\beta_1 = \frac{33 - 2n_f}{12}, \quad \beta_2 = \frac{153 - 19n_f}{24},$$

$$A^{(1)} = \frac{4}{3}, \quad A^{(2)} = \frac{67}{9} - \frac{\pi^2}{3} - \frac{10}{27}n_f + \frac{8}{3}\beta_1 \ln\left(\frac{e^{\gamma_E}}{2}\right), \quad (36)$$

where γ_E is the Euler constant.

Note that s is defined for $\hat{q} \geq \hat{b}$, and set to zero for $\hat{q} < \hat{b}$. As a similar treatment, the complete Sudakov factor $\exp(-S)$ is set to unity, if $\exp(-S) > 1$, in the numerical analysis. This corresponds to a truncation at large k_T , which spoils the on-shell requirement for the light valence quarks. The quark lines with large k_T should be absorbed into the hard scattering amplitude, instead of the wave functions. An explicit examination shows that the partial expression including only the first six terms gives predictions smaller than those from the full expression by less than 5% [2].

References

- [1] H.-n. Li and H.L. Yu, Phys. Rev. Lett. 74, 4388 (1995); Phys. Lett. B (1995); H.-n. Li, Phys. Lett. B348, 597 (1995).
- [2] H.-n. Li, Phys. Rev. D52, 3958 (1995).
- [3] H.-n. Li, preprint CCUTH-95-02.
- [4] H.-n. Li and H.L. Yu, preprint CCUTH-95-04.
- [5] F. Schlumpf, talk given at XIVth European Conference on Few-Body problems in Physics, Amsterdam, The Netherlands, 1993 (unpublished).
- [6] M.S. Alam *et al.* (CLEO Collaboration), Phys. Rev. D50, 43 (1994).
- [7] N. Isgur and M.B. Wise, Phys. Lett. B232, 113 (1989); 237, 527 (1990).
- [8] M. Neubert, Phys. Lett. B264, 455 (1991).
- [9] M. Neubert and V. Rieckert, Nucl. Phys. B382, 97 (1992).
- [10] A. Abd El-Hady, K.S. Gupta, A.J. Sommerer, J. Spence and J.P. Vary, Phys. Rev. D51, 5245 (1995).
- [11] B. Barish *et al.* (CLEO Collaboration), Phys. Rev. D51, 1014 (1995).
- [12] Review of Particle Properties, Phys. Rev. D50 (1994).
- [13] C. Bernard, talk presented at the CTEQ summer school on QCD analysis and phenomenology, Missouri, 1994 (unpublished); C. Bernard, J. Labrenz and A. Soni, Phys. Rev. D49, 2536 (1994).
- [14] D. Bortoletto and S. Stone, Phys. Rev. Lett. 65, 2951 (1990).
- [15] K. Berkelman and S. Stone, Annu. Rev. Nucl. Part. Sci. 41, 1 (1991).
- [16] M. Bauer, B. Stech and M. Wirbel, Z. Phys. C29, 637 (1985); 34, 103 (1987).
- [17] A. Abada *et al.*, Nucl. Phys. B376, 172 (1992); M. Neubert, Phys. Rev. D46, 1076 (1992).
- [18] C.G. Boyd, B. Grinstein and R.F. Lebed, Phys. Lett. B353, 306 (1995).

- [19] M. Neubert, Phys. Rep. 245, 261 (1994); Z. Ligeti, Y. Nir and M. Neubert, Phys. Rev. D49, 1302 (1994).
- [20] M. Shifman, N. Uraltsev and A. Vainshtein, University of Minnesota Report No. TPI-MINN-94/13-T (unpublished).
- [21] T. Mannel, Phys. Rev. D50, 428 (1994).
- [22] C.A. Dominguez, in Proceedings of the Third Workshop on the Tau-Charm Factory, Spain (1993).
- [23] R.J. Oakes, Phys. Rev. Lett. 73, 381 (1994).
- [24] C.Y. Wu, T.W. Yeh and H.-n. Li, in preparation.
- [25] J.G. Körner and G.A. Schuler, Z. Phys. C38, 511 (1989).
- [26] N. Isgur, D. Scora, B. Grinstein and M.B. Wise, Phys. Rev. D39, 799 (1989).
- [27] H.-n. Li and G. Sterman, Nucl. Phys. B381, 129 (1992); H.-n. Li, Phys. Rev. D48, 4243 (1993).

Figure Captions

Fig. 1. (a) Factorization of $B \rightarrow D^{(*)}$ transitions. (b) $\mathcal{O}(\alpha_s)$ corrections to wave functions.

Fig. 2. Dependence of the B and $D^{(*)}$ meson wave functions on the momentum fraction x .

Fig. 3. The spectrum $d\Gamma/dq^2$ of the semileptonic decay $\bar{B}^0 \rightarrow D^{*+}\ell^-\bar{\nu}$.

Fig. 4. Dependence of ξ_+ and ξ_{A_1} on the cutoff b_c for $\eta = 1.3$.

Fig. 5. Dependence of (a) ξ_+ , ξ_V , ξ_{A_1} and ξ_{A_3} and of (b) ξ_- and ξ_{A_2} on η .

Fig. 6. Dependence on η of (1) eq. (29), (2) eq. (28), (3) eq. (30), (4) eq. (27) for the linear fit with $\mathcal{F}(1) = 0.93$, and (5) eq. (27) for the quadratic fit with $\mathcal{F}(1) = 0.93$. The curves of ξ_+ and ξ_V are also shown.

Fig. 7. (a) W -exchange and (b) internal W -emission $\mathcal{O}(\alpha_s)$ diagrams.

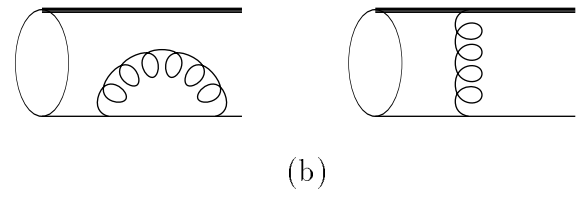
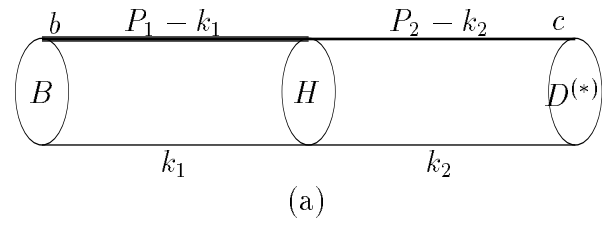


Figure 1

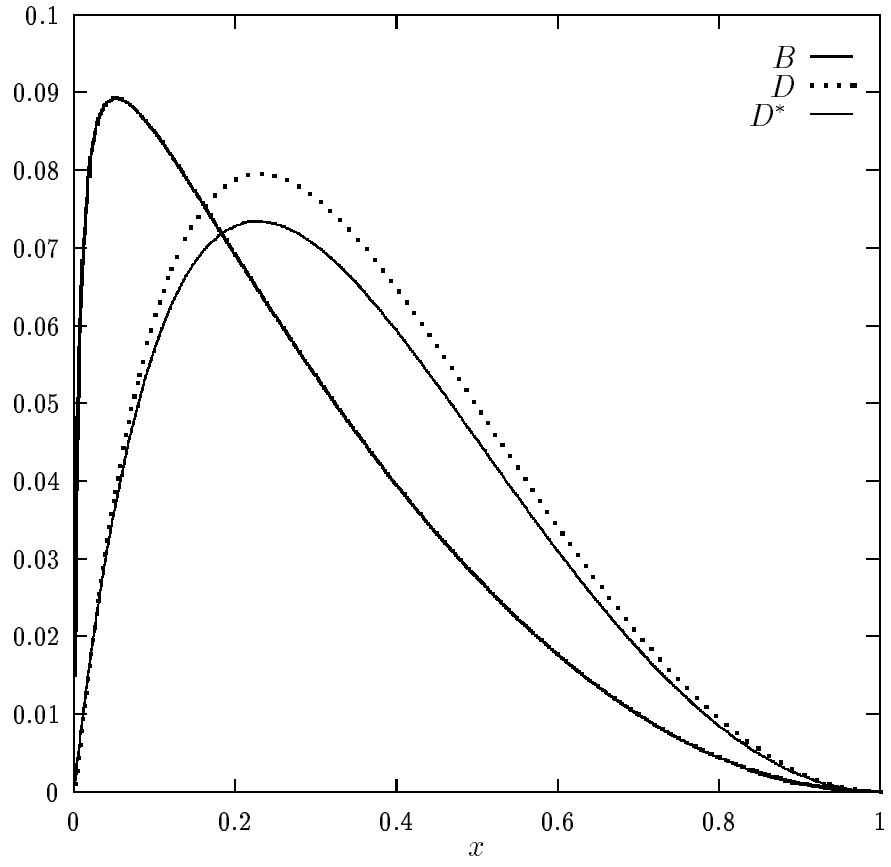


Figure 2

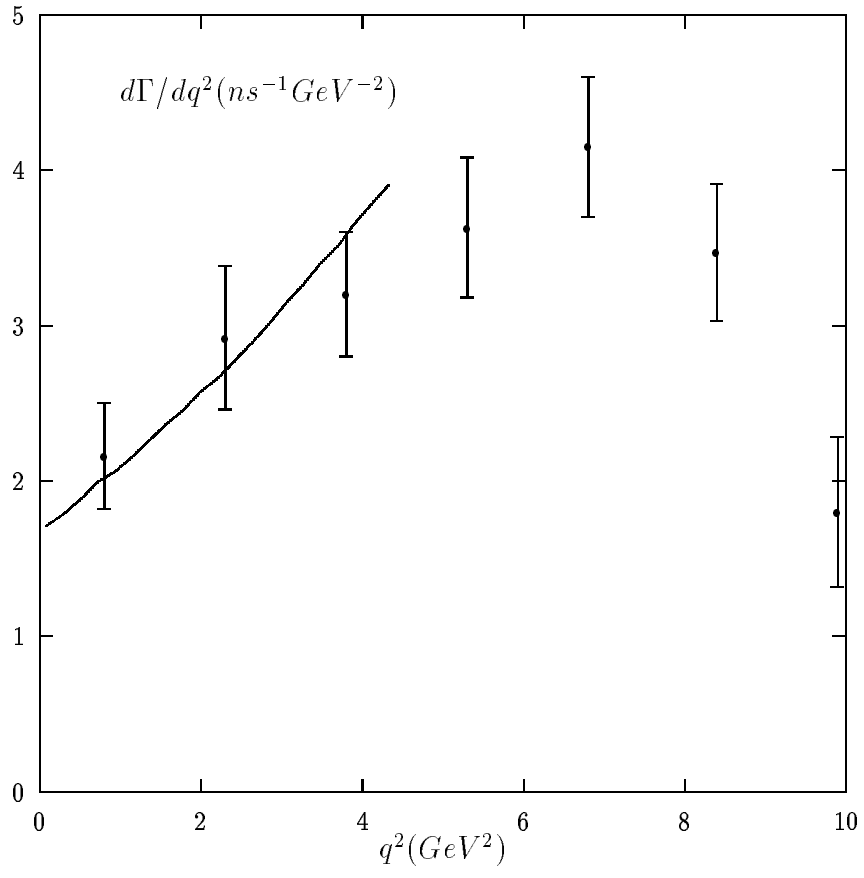


Figure 3

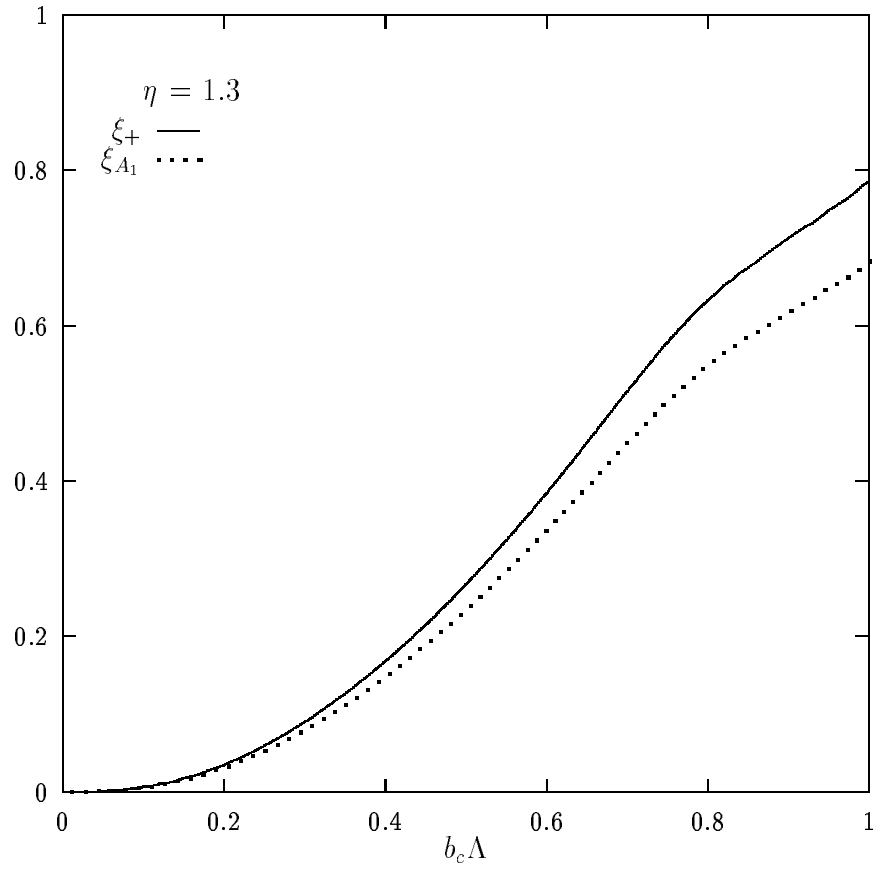


Figure 4

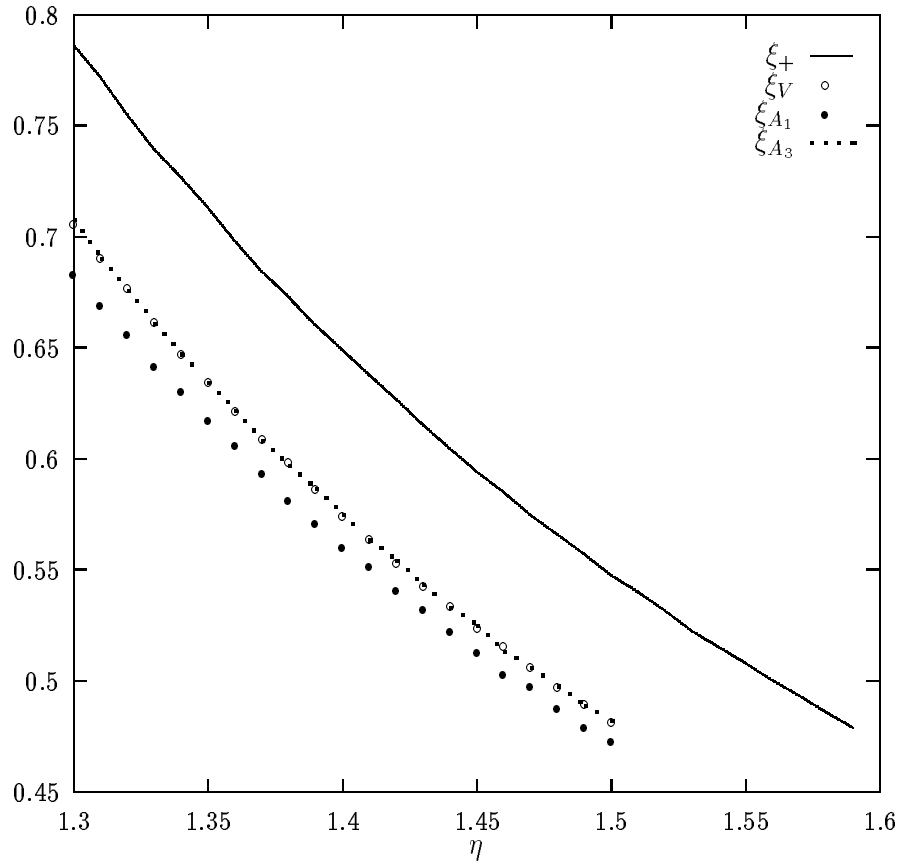


Figure 5a

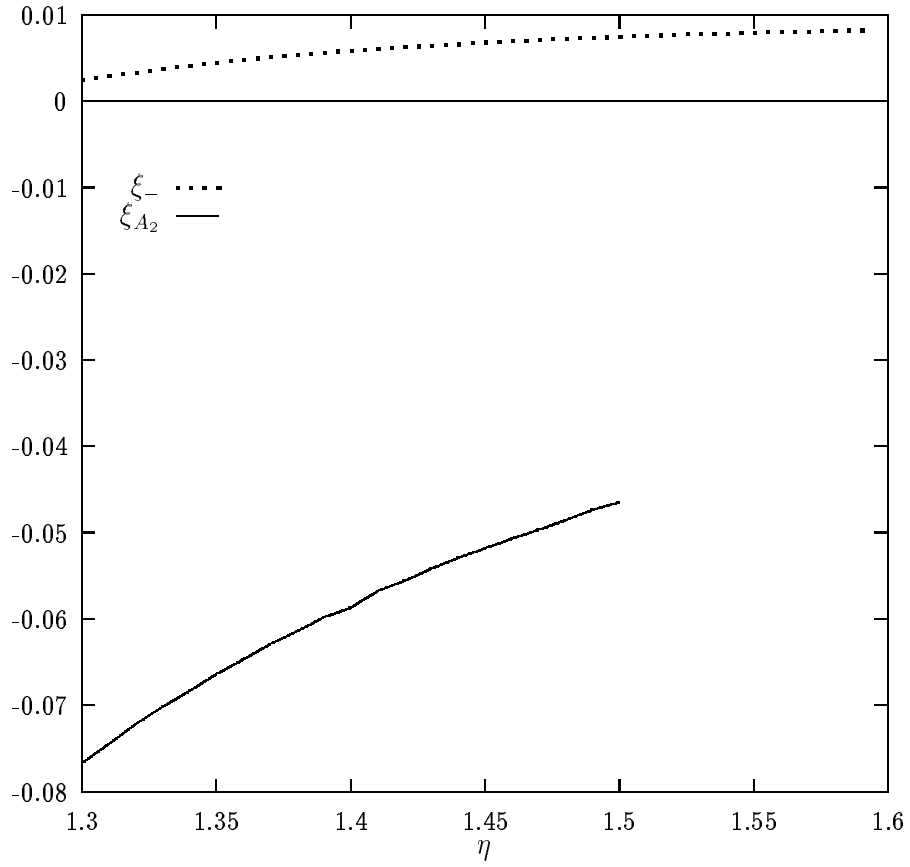


Figure 5b

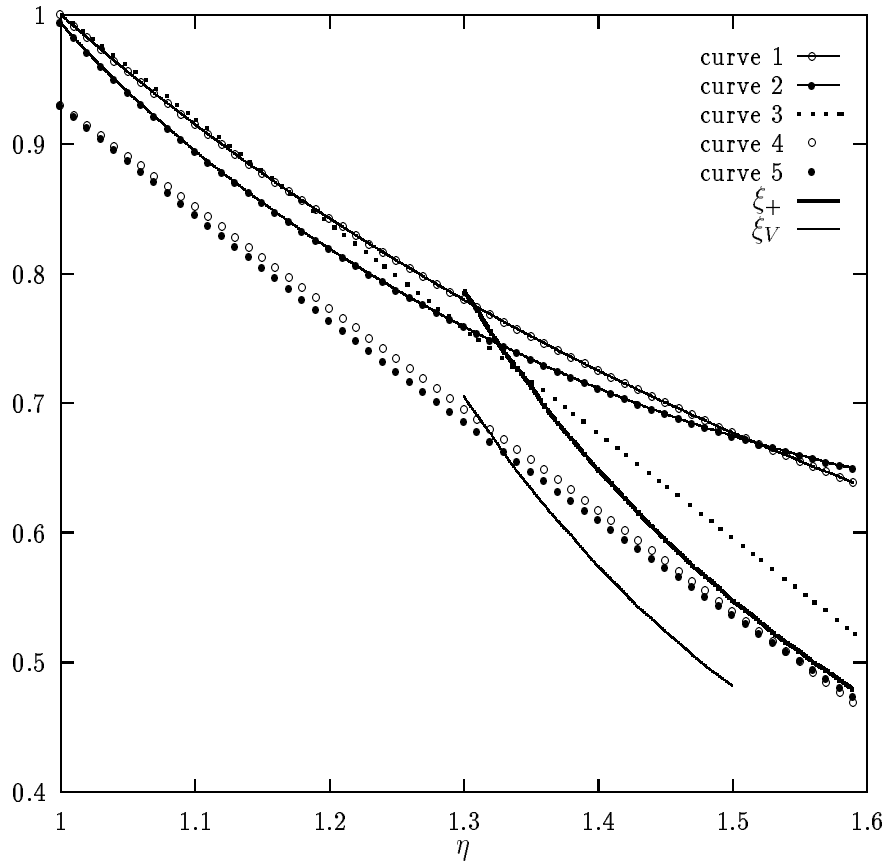
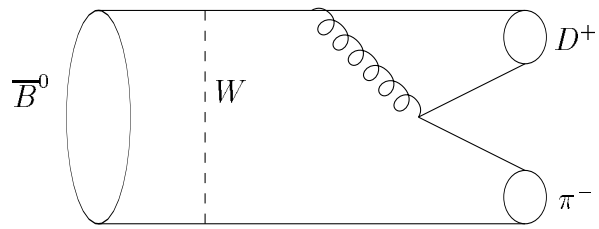
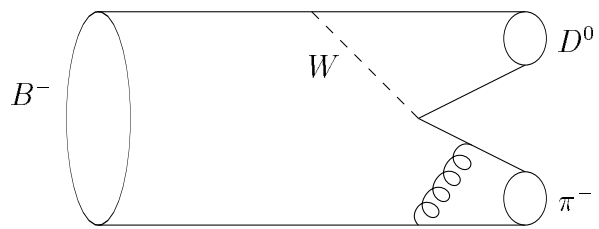


Figure 6



(a)



(b)

Figure 7